

# Detection and Phenotyping of Retinal Disease using AM-FM Processing for Feature Extraction

Carla Agurto<sup>1</sup>, Sergio Murillo<sup>1</sup>, Victor Murray<sup>1</sup>, Marios Pattichis<sup>1</sup>, Stephen Russell<sup>2</sup>, Michael Abramoff<sup>2</sup> and Pete Soliz<sup>2,3</sup>

<sup>1</sup>University of New Mexico, Department of Electrical and Computer Engineering  
Albuquerque, NM 87131, USA

<sup>2</sup>University of Iowa, Department of Ophthalmology and Visual Sciences  
Iowa City, IA 52242, USA

<sup>3</sup>VisionQuest  
Albuquerque, NM 87109, USA

**Abstract-** We present the application of an Amplitude-Modulation Frequency-Modulation (AM-FM) method for extracting potentially relevant features towards the classification of diseased retinas from healthy retinas. In terms of AM-FM features, we use histograms of the instantaneous amplitude, the angle of the instantaneous frequency and the magnitude of the instantaneous frequency extracted over different frequency scales. To classify the AM-FM features, we use a combination of a clustering method and Partial Least Squares (PLS). Using 18 images from each of the four risk levels, three experiments were performed to test the algorithm's ability to differentiate the controls (Risk 0) from each of the three levels of pathology, i.e. Risk 1, Risk 2, and Risk 3. For Risk 0 versus Risk 3 an area under the receiver operating system (AROC) of 0.99 was achieved with a best sensitivity of 100% and a specificity of 95%. For Risk 0 versus Risk 2, the AROC was 0.96 with 94% sensitivity and 85% specificity. For Risk 0 versus Risk 1, the AROC was 0.93 and a sensitivity/specificity of 94%/67%.

## I. INTRODUCTION

Surveys of Diabetic Retinopathy (DR) have shown that this disease is the most common cause of blindness in the USA. Furthermore only 10% of all the acquired retina images are diseased and require treatment [1]. The proposed computer-based methodology for DR Screening depends less on lesion by lesion segmentation or detection, as do most other approaches that have been reported [2]-[4].

Previously published studies have required a pre-processing step in order to make detection of the lesions possible. Osareh et al. [5] used color normalization and local contrast enhancement as an initial step for detecting exudates. Flemming et al. [6] applied a 3x3 pixel median filter to reduce the noise. They convolved the image with a Gaussian filter and then applied normalization to the image for the detection of exudates. Niemeijer et al. [3] also performed pre-processing to the retinal image. They followed the same pre-processing steps proposed by Spencer et al. [7] and Frame et al. [8]. This method consists of removing the slow gradients in the background of the green channel of each image resulting in a shade corrected image. Other approaches are focused on the development of pre-processing steps for the detection and subsequent removal of normal anatomical

structures in the image. The most common methods segment retinal vessels which have the same intensity levels as red lesions [9], [10]. Our method, similar to Niemeijer et al. [4], does not require any preprocessing. The green channel of the image is the input for applying the feature extraction processing.

For feature extraction, previous methods include the application of Morphological methods [11], Gabor filters [12], Wavelet transforms [13] and Matched filters [14]. The latter have been widely used on retinal images for vessels segmentation. The extracted features are often presented as histograms, where high-order statistics, such as skewness, and kurtosis, are calculated for additional features.

In our proposed approach, we consider the extraction of Amplitude-Modulation Frequency-Modulation (AM-FM) features for image classification. We refer to [15] for a related application in retinal image analysis and content-based image retrieval. Furthermore, we refer to [16] for further details on the general AM-FM methodology for digital image and video processing. AM-FM models allow us to model both continuous-scale and discontinuous variations in digital images. AM-FM models have been applied to several image analysis tasks. Pattichis et al used AM-FM models to segment different structures from digital images from electron microscopic muscle imaging [17]. For a more analytical treatment of FM analysis we refer to [18]. For AM-FM applications in medical video motion analysis and image segmentation we refer to [18,19].

In section II, the methodology used in this approach is explained. In this part, the database used to test this approach as well the steps for the classification are detailed. Results are provided in section III. Finally the discussion and conclusions are in section IV and V respectively.

## II. METHODOLOGY

### A. Database

Seventy-two images (18 from each one of four levels) were selected for this study to evaluate the AM-FM features as a means for detecting DR in retinal images. The levels of DR were defined by the Service Ophtalmologie Lariboisière [21].

TABLE I  
SUMMARY OF DIABETIC RETINOPATHY DATABASE.

RETINOPATHY GRADE	
Risk	Number of images
3	149
2	70
1	30
0	151
total	400

The most severe level of DR is grade 3, in which 15 or more microaneurysms are present. For grade 2, the number of microaneurysms in the retina is between 5 and 15 and for grade 1 the retinal images contain between 1 and 5 microaneurysms. The grade 0 corresponds to diabetic patients with no apparent DR in the image. It is important to mention that the images not only contain red lesions such as microaneurysms and hemorrhages, but also contain bright lesions such as exudates and cotton-wool spots.

These 72 images were chosen randomly from a group of 400 images whose characteristics are shown in table I. Note that all the data were extracted from the MESSIDOR database [20].

### B. Fundus Photography

For this study, all the retinal images are in color and were captured using 8 bits per plane and a resolution of 2240x1488 pixels. Images were acquired using a 3CCD camera on a Topcon TRC NW6 with a 45 degree field of view. These 72 images were taken with pupil dilation (one drop of Tropicamide at 10%) and were stored in a TIF format.

### C. Feature Extraction.

An AM-FM method was used to extract the features for the classification. An image is modeled as a sum of AM-FM harmonics. We write

$$I(x, y) = \sum_{n=1}^M a_n(x, y) \cos \phi_n(x, y) \quad (1)$$

where  $a_n(x, y)$  denotes slowly-varying amplitude functions and  $\phi_n(x, y)$  denotes the phase functions. For each instantaneous phase function, we associate the instantaneous frequency (IF) using:

$$\nabla \phi_n(x, y) = \left( \frac{\partial \phi_n(x, y)}{\partial x}, \frac{\partial \phi_n(x, y)}{\partial y} \right) \quad (2)$$

The Instantaneous Frequency (IF) represents a vector field which allows us to model variations in local image orientation in terms of the direction of the IF vectors. We demonstrate an example of the dependency of the angle of the IF in Fig. 1. Here, we note that the Instantaneous Frequency magnitude remains invariant to any rotations. The IF magnitude depends on the local geometric structure. It is less sensitive on slowly-varying brightness variations.

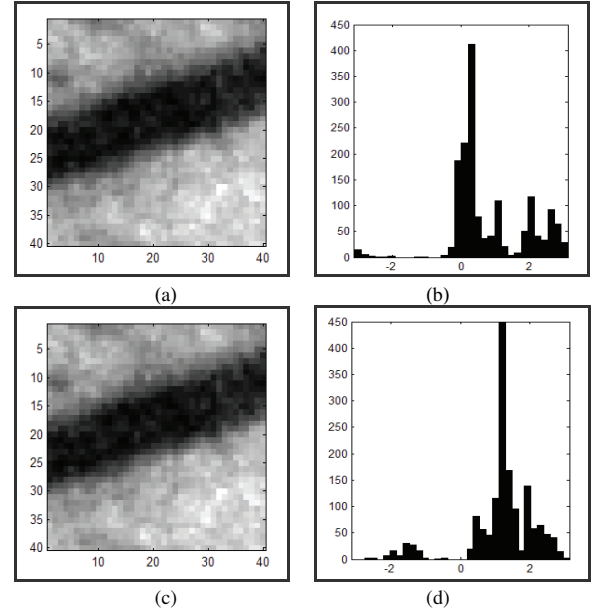


Fig. 1. Instantaneous Frequency angle estimate for two vessel regions. (a) horizontally-rotated vessel, (b) histogram for the angle estimate of the instantaneous frequency for low and medium frequencies (see filters 8-19 in Fig. 2) of (a), (c) vertically-rotated vessel, (d) histogram for the angle estimate of the instantaneous frequency for low and medium frequencies of (c).

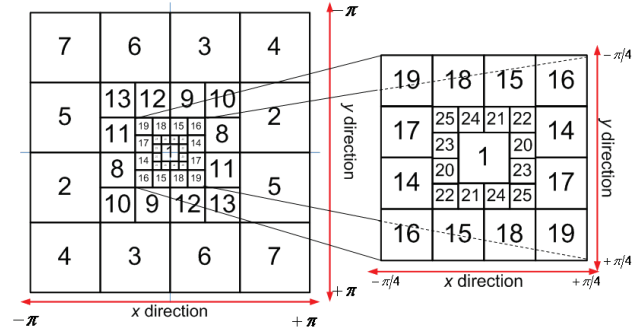


Fig. 2. Separable Filterbank for AM-FM Analysis. On the right, we zoom into the lower-frequency bands.

TABLE II  
FREQUENCY CLASSIFICATION FOR BANDPASS FILTERS (SEE FIG. 2).

Group	Filters	Frequency Range
1	1	Low Pass Filter
2	From 20 to 25	Very Low frequencies (VL)
3	From 14 to 19	Low frequencies (L)
4	From 8 to 13	Medium frequencies (M)
5	From 14 to 25	L + VL
6	From 8 to 19	M + L
7	From 8 to 25	M+L+VL

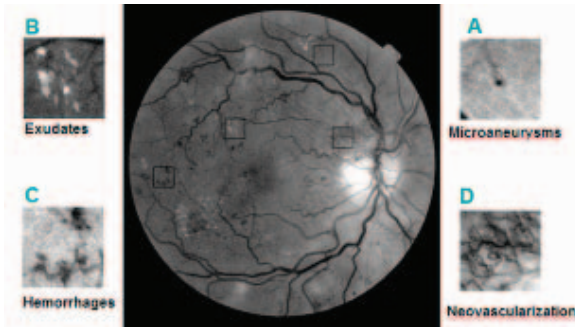


Fig. 3. Lesions presented in a DR retinal image.

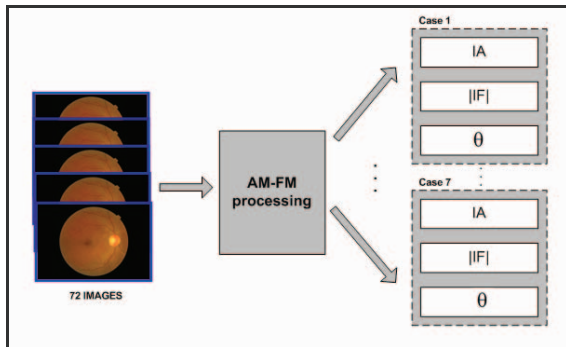


Fig. 4. Feature extraction using AM-FM.

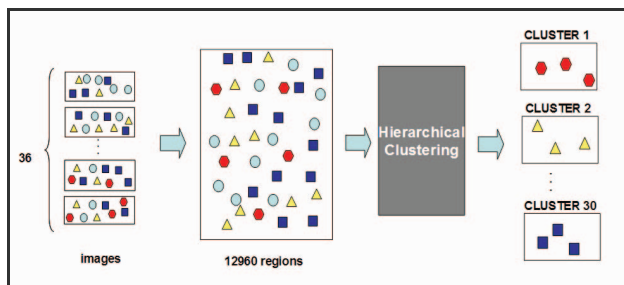


Fig. 5. Hierarchical Clustering. First, the information from all the regions in the 36 images is grouped (12960 regions). Then, a hierarchical clustering is applied to group the information of the regions in 30 clusters.

TABLE III

IMAGE REPRESENTATION IN TERMS OF CLUSTER MEMBERSHIP. FOR EACH CLUSTER, WE COUNT THE NUMBER OF TIMES THAT AN IMAGE FEATURE (FROM EACH ROI) IS CLASSIFIED IN EACH CLUSTER.

TYPE	IMAGES	CLUSTER 1	CLUSTER 2	CLUSTER 3	...	CLUSTER 30
NON DR	1	0	15	10	...	23
NON DR	2	1	10	10	...	19
	3	0	12	7	...	20
	...	...	...	...	...	...
DR	35	5	9	12	...	23
DR	36	8	11	13	...	25

We perform AM-FM demodulation over different frequency bands, after applying a filterbank. We present the frequency-domain filterbank decomposition in Fig. 2. We

then apply Dominant Component Analysis (DCA) to estimate the dominant AM-FM component over different groups of filters (see Table II). We considered seven different groups as detailed in Table II. For details on the AM-FM demodulation procedure we refer to [15,16].

Over each filter group, we estimate the instantaneous amplitude and the instantaneous frequency. For image classification, we use the histograms of (i) the instantaneous amplitude, (ii) the instantaneous frequency angle (where the most frequent value was shifted to zero, centering the histogram around zero) and (iii) the instantaneous frequency magnitude. We thus compute three histograms for each one of our seven groups, giving a total of twenty-one histograms.

For our approach, a region of 960x600 pixels in the retina is selected for each image. This region was positioned besides the optic nerve in which usually the lesions appear. Since many of the lesions present in a diseased retina are on the order of few pixels (~10 pixels) and AM-FM is a pixel based technique the region is divided into 360 sub-regions of 40x40 pixels. These 40x40 pixels sub-regions allow an analysis of the smaller lesions as well as the larger lesions

A 40-bin histogram is calculated for each of the 21 histograms (7 groups of 3 histograms each) giving a total of 840 features obtained per region. For each experiment, we use 18 images of grade 0 and 18 images from grades 1, 2 or 3. The feature matrix per experiment (36 images) is composed of 12960 regions x 840 features. To reduce the dimensionality of the feature set, we use Principal Components Analysis (PCA). With the PCA method, we used the principal projections that explained 95% of the variance (or more).

#### D. Unsupervised classification

Once the features per region and per case were obtained, a clustering method was used as a pre-classification step. Since the goal of this method is to find differences between healthy and diseased retinal images that could contain any kind of structure (see Fig. 3), hierarchical clustering approach was used. The objective of this step was to cluster regions according to the characteristics of the IA and |IF| and angle histograms. Some of the clusters correspond to regions that appeared with some form of DR pathology. Other clusters represent regions with normal anatomical structures such vessels and yet other regions are characterized by a mixture of normal and abnormal structures. Fig. 4 shows how the different structures found in each image are grouped in different clusters.

This method, unlike other unsupervised methods, groups the regions that have common features and the clustering is performed in a tree structure form so that depending on the application a different hierarchical level is used for the clustering. In this approach 30 clusters are used for the classification.

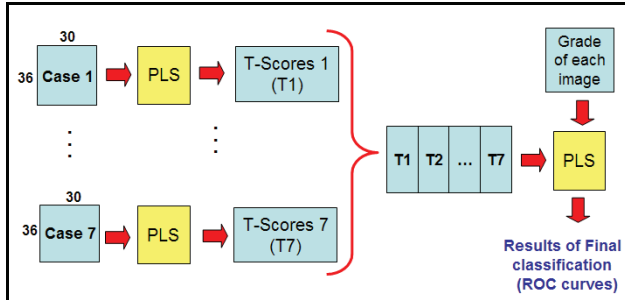


Fig. 6. Two-step classification using Partial Least Squares (PLS).

### E. Supervised Classification.

After the clustering was performed, a new matrix per image containing the cluster information per image was found (see Fig. 5). Note also that the matrix of analysis is  $36 \times 30$ , where 36 represents the images in our experiment and 30 are the new features obtained with the hierarchical clustering. Now that a new information matrix per image is obtained and the class of each image has been given by medical experts, a supervised method called Partial Least Squares (PLS) is applied. This linear regression method widely used in various disciplines such as chemistry, economics, medicine, etc. has two principal algorithms: Nonlinear iterative partial least squares (NIPALS) and SIMPLS (Jong 1993). The latter algorithm is used for the final classification. To obtain the best performance of the algorithm, the classification is performed in two steps as it is shown in Fig. 6.

In the first part, the PLS algorithm is applied using the information provided for each of the 7 groups. In this classification method, the data is decomposed into 2 matrices (T-scores and Loading matrix). The T-scores, which depend of the number of factors, were used as the new matrix for the classification (See Fig. 6). Depending of the number of factors, a different prediction in the classification was obtained. To improve the classification, the T-scores that gave the best area under the ROC curve (AROC) using jackknife were combined to compose a new matrix. Once the matrix of the T-scores for each of the 7 groups are concatenated, the PLS is applied again. For this second run of the PLS algorithm, the number of factor that gave the best AROC is sought. After the best AROC is found, the optimal number of factors is used to find the predictors for the classification. Again this was accomplished using the jackknife approach. Finally, the ROC curve is plotted using the predictors and the ground truth.

### III. RESULTS

We summarize the results using the ROC curves in Figs 7-9. Fig. 7 shows the ROC curve for the Risk 3 vs. Risk 0. The area under the curve of the classification of the retinal images for the first experiments (risk3 vs. risk0) is 0.99. This approach achieved best sensitivity/specificity of 100%/95%. Fig. 8 shows the ROC curve for the Risk 2 vs. Risk 0. The area under the curve for this classification is 0.96 and its best sensitivity/specificity is 100%/78% or 94%/85%. Finally,

Fig. 9 shows the ROC curve for the case of the Risk 1 vs. Risk 0 using 2 factors. This approach achieved an area of 0.93 under the curve and a sensitivity/specificity of 94%/67%.

### IV. DISCUSSION

The principal contribution of this research was to demonstrate a means for screening digital images for DR without the need to train on a set of images where each type of lesion associated with DR was marked by an ophthalmologist or trained analyst. The high sensitivities and specificities that have been achieved are encouragement to test this methodology on the remaining 1100 images in the MESSIDOR database and apply the technique to other available databases.

In the analysis of the hierarchical clustering, we found that there is a potential for identifying the specific region that indicates where pathology has been located, but without explicit segmentation of the pathology. The process is computationally efficient and can be implemented for on-site “real-time” screening, as well as for a tool for off-site and non-real-time analysis such as one might encounter in a research study. The quantitative nature of the results lends itself for highly objective studies of large databases.

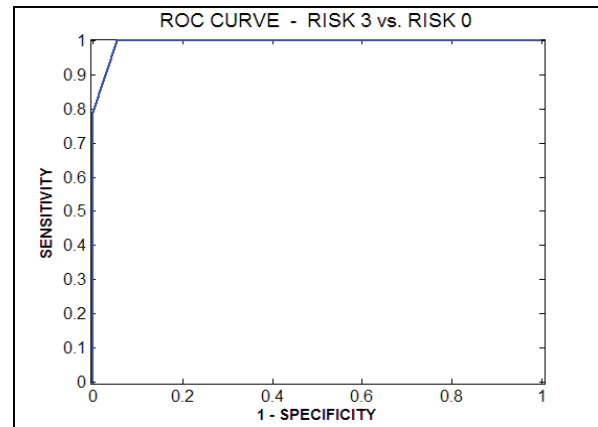


Fig. 7. ROC curve for Risk 3 vs. Risk 0.

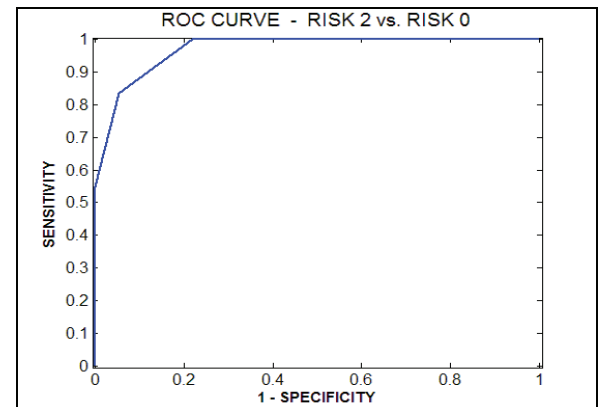


Fig. 8. ROC curve for Risk 2 vs. Risk 0.

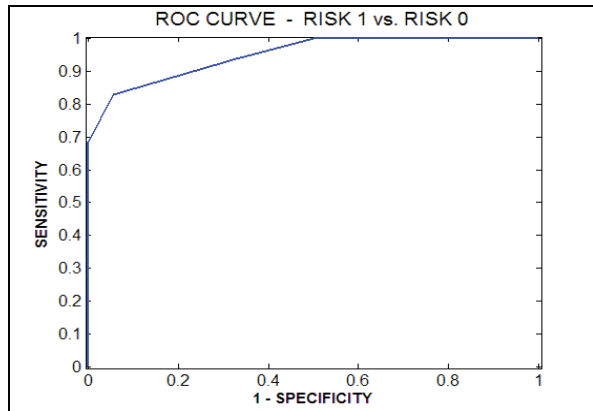


Fig. 9. ROC curve for Risk 1 vs. Risk 0.

### V. CONCLUSION

The use of AM-FM features for distinguishing between the different grades of diabetic retinopathy gave excellent, preliminary results. An advantage of the AM-FM approach lies in the fact that it did not require pre-processing or any type of segmentation prior to feature extraction. We expect that we will also have excellent results in applying the proposed techniques over much larger databases of retinal images.

### VI. ACKNOWLEDGMENTS

National Institute of Health (NIH) Phase I grant number 1R44EY018280-01A1 titled "Computer based screening for diabetic retinopathy" and Méthodes d'Evaluation de Systèmes de Segmentation et d'Indexation Dédiées à l'Ophthalmologie Rétinienne (MESSIDOR) for providing the database.

### REFERENCES

[1] M. D. Abramoff and M. S. A. Suttorp-Schulten, "Web-based screening for diabetic retinopathy in a primary care population: the eyecheck project," *Telemed J E Health*, vol. 11, no. 6, pp. 668-674, Dec 2005.

[2] M. Larsen, J. Godt, N. Larsen, H. Lund-Andersen, A. K. Sjølie, E. Agardh, H. Kalm, M. Grunkin, and D. R. Owens, "Automated detection of fundus photographic red lesions in diabetic retinopathy," *Investigat. Ophth & Vis. Sci.*, vol. 44, no. 2, pp. 761-766, 2003.

[3] M. Niemeijer, B. van Ginneken, S.R. Russel, M.S.A. Suttorp-Schulten, M.D. Abramoff, "Automated detection and differentiation of Drusen, exudates, and cotton-wool spots in digital color fundus photographs for early diagnosis of Diabetic Retinopathy", *Investigat. Ophth & Vis. Sci.*, vol. 48, pp. 2260-2267, 2007.

[4] M. Niemeijer, B. van Ginneken, J. J. Staal, M. S. A. Suttorp-Schulten and M. D. Abramoff "Automatic detection of red lesions in digital color fundus photographs," *IEEE Trans. Med. Imag.*, vol. 24, pp. 584, May 2005.

[5] A. Osareh, M. Mirmehdi, B. Thomas, and R. Markham, "Automated Identification of Diabetic Retinal Exudates in Digital Colour Images," *British Journal of Ophthalmology*, vol. 87, pp. 1220-1223, 2003.

[6] Alan D Fleming, Sam Philip, Keith A Goatman, Graeme J Williams, John A Olson and Peter F Sharp, "Automated detection

of exudates for diabetic retinopathy screening," *Phys. Med. Biol.*, vol. 52 pp. 7385-7396, 2007

[7] T. Spencer, J. A. Olson, K. C. McHardy, P. F. Sharp, and J. V. Forrester, "An image-processing strategy for the segmentation and quantification of microaneurysms in fluorescein angiograms of the ocular fundus," *Comput. Biomed. Res.*, vol. 29, no. 4, pp. 284-302, 1996.

[8] J. Frame, P. E. Undrill, M. J. Cree, J. A. Olson, K. C. McHardy, P. F. Sharp, and J. V. Forrester, "A comparison of computer based classification methods applied to the detection of microaneurysms in ophthalmic fluorescein angiograms," *Comput. Biol. Med.*, vol. 28, no. 3, pp. 225-238, 1998.

[9] Ricci, E.; Perfetti, R., "Retinal Blood Vessel Segmentation Using Line Operators and Support Vector Classification," *IEEE Trans. On Medical Imaging*, vol.26, no.10, pp.1357-1365, Oct. 2007.

[10] J. J. Staal, M. D. Abramoff, M. Niemeijer, M. A. Viergever and B. van Ginneken "Ridge based vessel segmentation in color images of the retina," *IEEE Trans. Med. Imag.*, vol. 23, pp. 501-509, Apr. 2004.

[11] T. Walter and J. C. Klein, "Segmentation of color fundus images of the human retina: Detection of the optic disc and the vascular tree using morphological techniques," in *Medical Data Analysis*, J. Crespo, V. Majojo, and F. Martin, Eds. Berlin, Germany: Springer-Verlag, 2001, pp. 282-287. ser. Lecture Notes in Computer Science.

[12] D. Vallabha, R. Dorairaj, K. Namuduri and H. Thompson, "Automated detection and classification of vascular abnormalities in diabetic retinopathy," in *Proc. 38<sup>th</sup> Asilomar Conf. on Signals, Systems and Computers*, vol.2, no. 7-10, pp. 1625-1629, Nov. 2004.

[13] G. Quellec, M. Lamard, P.M. Josselin, G. Cazuguel, B. Cochener and C. Roux, "Optimal Wavelet Transform for the Detection of Microaneurysms in Retina Photographs," *IEEE Trans. On Medical Imaging*, vol.27, no. 9, pp.1230-1241, Sept. 2008

[14] M. Al-Rawi, M. Qutaishat and M. Arrar, "An improved matched filter for blood vessel detection of digital retinal images", *Computers in Biology and Medicine*, vol. 37, no. 2, pp. 262-267, 2007.

[15] V. Murray, M.S. Pattichis M.S. and P. Soliz, "New AM-FM analysis methods for retinal image characterization", in *Proc. 42<sup>nd</sup> Asilomar Conf. on Signals, Systems and Computers*, 2008.

[16] Victor Manuel Murray Herrera, "AM-FM methods for image and video processing," Ph.D. dissertation, University of New Mexico, September 2008.

[17] M.S. Pattichis, C.S. Pattichis, M. Avraam, A.C. Bovik and K. Kyriacou, "AM-FM texture segmentation in electron microscopic muscle imaging," *IEEE Trans. On Med. Imaging*, vol. 19, no. 12, pp. 1253-1257, Dec. 2000.

[18] M.S. Pattichis and A.C. Bovik, "Analyzing image flow by multidimensional frequency modulation," *IEEE Trans. on Pattern Analysis and Machine Intelligence*, vol. 29, no. 5, pp. 753-766, 2007.

[19] V. Murray, S.E. Murillo, M.S. Pattichis, C.P. Loizou, C.S. Pattichis, E. Kyriacou, A. Nicolaides, "An AM-FM model for Motion Estimation in Atherosclerotic Plaque Videos," in *Proc. 41<sup>st</sup> Asilomar Conf. on Signals, Systems and Computers*, vol. 4, pp. 746-750, Nov. 2007.

[20] P. Rodriguez, V., M.S. Pattichis and M.B. Goens, "M-mode echocardiography image and video segmentation based on am-fm demodulation techniques," in *Proc. 25<sup>th</sup> Conf. of IEEE Engineering in Medicine and Biology Society*, vol.2, pp. 1176-1179, Sept. 2003.

[21] TECHNO-VISION Project, "MESSIDOR: methods to evaluate segmentation and indexing techniques in the field of retinal ophthalmology." [Online]. Available: <http://messidor.crihan.fr/>.